Are your MRI contrast agents cost-effective?
Learn more about generic Gadolinium-Based Contrast Agents.
FRESENIUS KABI
caring for life

AJNR

Prediction of Disease-Free Survival in Patients with Squamous Cell Carcinomas of the Head and Neck Using Dynamic Contrast-Enhanced MR Imaging

S. Chawla, S. Kim, L.A. Loevner, W.-T. Hwang, G. Weinstein, A. Chalian, H. Quon and H. Poptani

This information is current as of April 17, 2024.

AJNR Am J Neuroradiol 2011, 32 (4) 778-784
doi: https://doi.org/10.3174/ajnr.A2376
http://www.ajnr.org/content/32/4/778

ORIGINAL RESEARCH

S. Chawla
S. Kim
L.A. Loevner
W.-T. Hwang
G. Weinstein
A. Chalian
H. Quon
H. Poptani

FELLOWS' JOURNAL CLUB

Prediction of Disease-Free Survival in Patients with Squamous Cell Carcinomas of the Head and Neck Using Dynamic Contrast-Enhanced MR Imaging

BACKGROUND AND PURPOSE: Patients with HNSCC have a poor prognosis and development of imaging biomarkers that predict long-term outcome might aid in planning optimal treatment strategies. Therefore, the purpose of the present study was to predict disease-free survival in patients with HNSCC by using pretreatment K^{trans} measured from dynamic contrast-enhanced MR imaging.

MATERIALS AND METHODS: Sixty-six patients with HNSCC were recruited from January 2005 to October 2008. Three patients were excluded because they underwent upfront neck dissection, and 6 patients were excluded due to suboptimal MR imaging data or being lost to follow-up. Disease-free survival was measured in the remaining 57 patients from the end date of chemoradiation therapy. In patients who died, the end point was the date of death, while in surviving patients the date of last clinical follow-up was used as the end point. Pretreatment K^{trans} and nodal volume were computed from the largest metastatic node, and median pretreatment K^{trans} and volume were used to divide patients into 2 groups (at or above the threshold value [group I] and below the threshold value [group II]. Disease-free survival was analyzed by the Kaplan-Meier method, and the results were compared by using a logrank test with K^{trans} and nodal volume as predictors. A P value $< .05$ was considered significant.

RESULTS: Thirteen of 57 patients had died of HNSCC by the last follow-up period (March 31, 2009). Patients with higher pretreatment K^{trans} values had prolonged disease-free survival compared with patients with lower K^{trans} values ($P = .029$). However, there was no significant difference in disease-free survival when nodal volume was used as a predictor ($P = .599$).

CONCLUSIONS: Pretreatment K^{trans} may be a useful prognostic marker in HNSCC.

ABBREVIATIONS: BW = bandwidth; CI = confidence interval; DCE-MRI = dynamic contrast-enhanced MR imaging; FA= flip angle; FDG = fluorodeoxyglucose; HNSCC = squamous cell carcinomas of the head and neck; K^{trans} = volume transfer constant; PET = positron-emission tomography; SUV = standard uptake value; TNM = Tumor, Node, Metastases

HNSCC remain a significant cause of mortality.[1] Despite advances in multidisciplinary management, the 5-year survival rate of patients with HNSCC has only improved marginally. A meta-analysis reported only 5% improvement in survival with induction chemotherapy compared with patients treated with surgery and/or radiation therapy alone.[2,3] The presence of metastatic cervical lymph nodes is considered a negative prognostic indicator in the treatment of HNSCC.[3,4] It has been reported that the presence of a single neoplastic neck node reduces the disease-free survival by 50% and that the presence of bilateral nodes further reduces the survival rate.[3,4] Consequently, assessment of the biology of nodal metastases is of prime importance and may aid in improving the clinical management of these patients. Development of noninvasive imaging biomarkers before initiation of treatment of HNSCC might assist in planning optimal treatment strategies, which may lead to a more favorable therapeutic outcome.

Patients with HNSCC with elevated tumor blood flow/blood volume respond more favorably to chemoradiation therapy than patients with low blood flow/volume.[5-9] DCE-MRI studies yield a parameter called K^{trans}, which is a measure of the first-order bidirectional volume transfer constant of contrast agent exchange between the intravascular plasma and tumor interstitium compartments. The pretreatment K^{trans}, which reflects tumor perfusion/permeability, has been shown to predict nodal treatment response to chemoradiation therapy in patients with HNSCC.[10] These studies imply that tumor vascularity may be an important predictor of local treatment response and disease control in HNSCC because elevated blood flow may permit improved delivery of therapeutic agents to the tumor. While other imaging modalities such as CT and PET have also been proposed for predicting prognosis and survival in patients with HNSCC,[6,11-13] lower soft tissue contrast and exposure to radiation associated with these modalities[14] call for an alternate imaging technique. Since DCE-MRI provides high temporal- and spatial-resolution maps of

Received May 3, 2010; accepted after revision August 20.

From the Departments of Radiology (S.C., S.K., L.A.L., H.P.), Biostatistics (W.-T.H.), Otorhinolaryngology (G.W., A.C.), and Radiation Oncology (H.Q.), University of Pennsylvania, Philadelphia, Pennsylvania; and Department of Radiology (S.K.), New York University, New York, New York.

This work was funded by the National Institutes of Health, grant R01-CA102756.

Please address correspondence to Harish Poptani, PhD, Research Associate Professor, University of Pennsylvania, B6 Blockley Hall, 423 Guardian Dr, Philadelphia, PA 19104; e-mail: poptanih@uphs.upenn.edu

Indicates open access to non-subscribers at www.ajnr.org

DOI 10.3174/ajnr.A2376

Demographics of patients with HNSCC

Characteristics	No. of Patients (N = 66)
Tumor location	
Base of tongue	26
Tonsil	16
Larynx	9
Vallecula	2
Nasopharynx	2
Oropharynx	2
Hypopharynx	1
Unknown primary	8
TNM staging	
TxN2M0	10
TxN3M0	3
T0N2M0	1
T1N2M0	2
T2N1M0	1
T2N2M0	17
T2N3M0	2
T3N2M0	10
T4N1M0	2
T4N2M0	16
T4N3M0	2

tissue perfusion/permeability, we evaluated the potential of pretreatment K^{trans} values from the metastatic lymph node in predicting disease-free survival (patients who survived a definite period of time without evidence of disease after chemoradiation therapy) in patients with HNSCC in this study.

Materials and Methods

Patients

This retrospective study was approved by the institutional review board, and written informed consent was obtained from each patient enrolled in the study. Patients were included in the study if they had prior CT/MR imaging examinations and biopsies confirming the presence of HNSCC on histopathology and had a metastatic cervical lymph node. Patients were excluded from the study if they had received any chemotherapy or radiation therapy previously, had any prior history of cancer other than HNSCC, had undergone upfront selective neck dissection, or had a major medical disorder such as poorly controlled diabetes mellitus or hypertension. On the basis of physical examinations and CT/MR imaging reports, all patients were assessed for the presence of metastatic cervical lymph nodes by a trained neuroradiologist and a radiation oncologist. In accordance with our inclusion criteria, the study initially comprised a cohort of 66 patients (mean age, 59.65 ± 10.37 years; 54 men and 12 women) newly diagnosed with HNSCC and recruited from January 2005 to October 2008. Tumor location and staging from these patients at initial presentation are summarized in the Table. The most common locations were the base of the tongue (40%), tonsil (25%), and larynx (14%). In 21% of patients, tumors were located on other less common sites or unknown sites. Three patients who underwent upfront neck dissection were excluded from the study. In addition, 6 patients were excluded from the data analysis because either the MR imaging data were corrupted from dental artifacts or these patients were lost to follow-up.

All patients were treated with chemoradiation therapy except for the 3 patients who elected to have upfront neck dissection. Patients were treated with a total dose of 7040 cGy in 32 fractions at a daily dose of 220 cGy per fraction, which was delivered for 44 days to the areas of gross disease. The chemotherapy regimen included either concurrent chemotherapy alone or induction chemotherapy followed by concurrent chemotherapy. Induction chemotherapy comprised 1–3 cycles of cisplatin (75 mg/m^2), docetaxol (75 mg/m^2), and 5-florouracil (1000 mg/m^2) or 8 cycles of cetuximab (400 mg), paclitaxel (90 mg), and carboplatin (155.1–239.8 mg). Concurrent chemotherapy comprised cisplatin (100 mg/m^2) or immunotherapy with 400 mg/m^2 of cetuximab 3–7 days before radiation therapy followed by weekly 250 mg/m^2 cetuximab on days 1, 8, 15, 22, 29, 36, and 43 of the radiation treatment.

Of the 57 patients who were finally included in the study, 33 (57.89%) did not undergo neck dissection, while 24/57 (42.11%) underwent neck dissection within 6 months after the end of chemoradiation therapy. Of these 24 patients, only 5 had viable lymph nodes on histopathology and 19 patients had biopsies negative for the presence of any viable carcinoma cells from the surgically removed lymph nodes.

Data Acquisition

All patients underwent MR imaging before surgery, radiation, or chemotherapy. The MR imaging study was performed by using a 1.5T Sonata scanner (Siemens, Erlangen, Germany) (n = 37) or a 3T Magnetom Trio scanner (Siemens) (n = 29). A neck array coil or a neurovascular coil was used for 1.5T and 3T scanners, respectively. The diagnostic and structural imaging protocol on both MR imaging systems included axial T2-weighted images (TR/TE = 4000/131 ms, FOV = 260 × 260 mm^2, matrix size = 384 × 512, section thickness = 5 mm, FA = 120°, BW = 130 Hz, NEX = 1), and axial T1-weighted images (TR/TE = 600/10 ms, FOV = 260 × 260 mm^2, matrix size = 384 × 512, section thickness = 5 mm, FA = 90°, BW = 130 Hz, NEX = 1). Eight axial sections with FOV = 260 × 260 mm^2 and section thickness = 5 mm were selected to cover the largest metastatic cervical lymph node for measurement with T1 and DCE-MRI.

The DCE-MRI protocol used in this study was described previously.[10,15] Briefly, DCE-MRI was performed by using a fast 3D spoiled gradient-echo sequence, which was modified to acquire 8 angle-interleaved subaperture images from the full-echo radial data.[16] Imaging parameters included the following: 256 readout points/view, 256 views (32 views/subaperture, 8 subapertures), FOV = 260 × 260 mm^2, 8 axial sections, section thickness = 5 mm, FA = 20°, receiver BW = 510 Hz/pixel, TR/TE = 5.0/4.2 ms. Fat saturation was applied once every 8 excitations. Spatial saturation was applied once every 32 excitations to minimize the flow effect while minimizing the scanning time. The scanning time of full-resolution data was approximately 20 seconds with fat and spatial saturations. This data-acquisition scheme resulted in a temporal resolution of 2.5 seconds for each subaperture image with full spatial resolution of 256 × 256 by using a dynamic k-space–weighted image reconstruction contrast algorithm. Baseline preinjection images were acquired for 1 minute. A single dose of gadodiamide (Gd-DTPA) (Omniscan; Nycomed, Oslo, Norway) at a concentration of 0.1 mmol/kg body weight was injected at the rate of 1 mL/s into the antecubital vein, followed by a saline flush with a power injector (Spectris; Medrad, Indianola, Pennsylvania), during which scanning was continued for another 9 minutes.

Image Processing

All images (T2, T1, postcontrast T1-weighted images, and DCE-MRI-derived K^{trans} maps) were coregistered by using a 2-step nonrigid image registration technique before data analysis based on the algo-

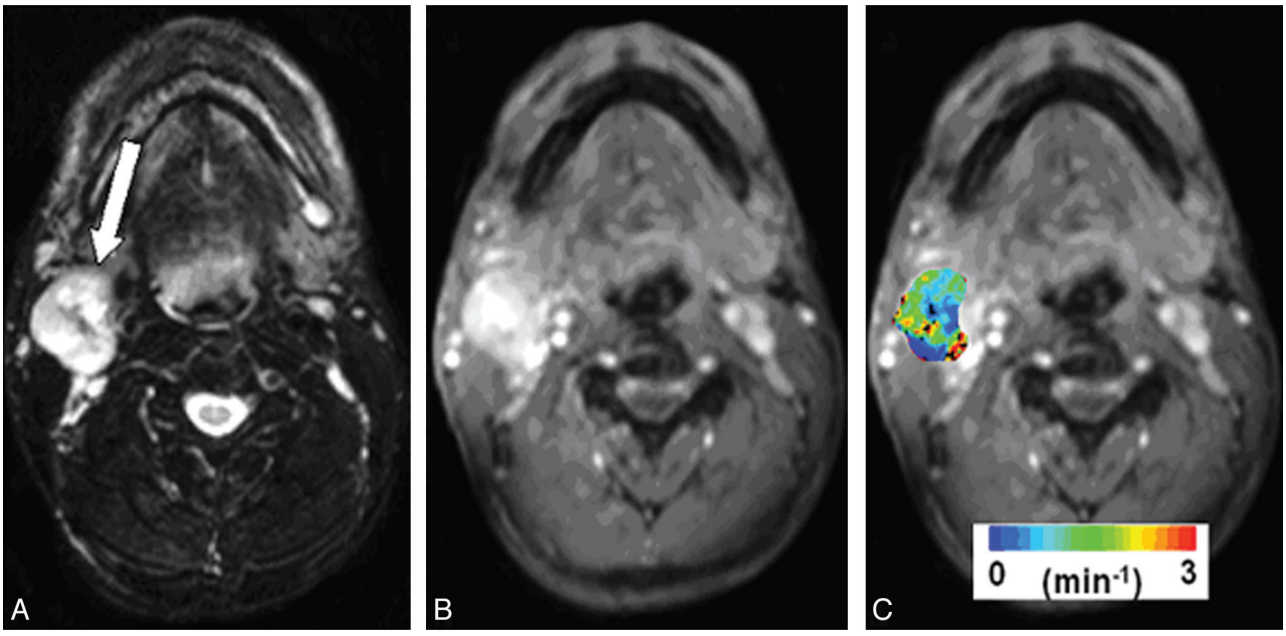

Fig 1. Representative images from a patient with HNSCC before chemoradiation therapy. *A,* Axial T2-weighted image demonstrates a heterogeneous hyperintense metastatic lymph node at level IIa of the right neck (*arrow*). *B,* This mass exhibits heterogeneous enhancement on a contrast-enhanced T1-weighted image. *C,* DCE-MRI–derived K^{trans} map is shown as a color image overlaid on a postcontrast T1-weighted image.

rithms described previously.[15,17] Regions of interest were drawn on the solid-appearing portion of the nodal mass by a trained neuroradiologist by using T2-weighted, T1-weighted, or postcontrast T1-weighted images, avoiding necrotic/cystic or hemorrhagic parts as well as surrounding blood vessels on all imaging sections encompassing the node. Pharmacokinetic analysis of the DCE-MRI data was performed for each voxel in the selected region of interest by using the shutter-speed model reported earlier.[10,15] These regions of interest were also used for the volumetric analysis.

Median pretreatment K^{trans} values were computed from the largest metastatic nodal mass by using only the central 4 sections to avoid erroneous results from wrap-around artifacts, typically observed on the end sections of the 3D images. Representative pretreatment structural MR images and a color-coded pharmacokinetic parametric K^{trans} map, overlaid on a postcontrast T1-weighted image from a patient, are shown in Fig 1.

Clinical Follow-Up and Data Analysis

The follow-up period was measured in 57 patients from the end date of chemoradiation therapy. Visits to physicians and laboratory, radiologic, or nuclear medicine reports were evaluated to find the date of last contact, and clinical records were studied to ascertain the cause of death. The clinical end point was the date of death from any cause in case of deceased patients and the time of last contact or date of last observation (March 31, 2009) in surviving patients. By the end of the last follow-up period, 17 of 57 (29.82%) patients had died. Of these 17 patients, 4 died of diseases unrelated to HNSCC (cardiac arrest, $n = 2$; respiratory failure, $n = 1$; and broken neck, $n = 1$) and were thus censored from the disease-free survival analysis. The remaining 13 patients died of HNSCC. The median follow-up for the surviving patients ($n = 40$) was 30 months (range, 13–48 months).

In the absence of an established cutoff value, the median pretreatment K^{trans} and volume from the metastatic nodal mass were considered as threshold values to separate the patients into 2 groups (at or above the threshold value [group I] and below the threshold value [group II]). Using K^{trans} and nodal volume as predictors, we estimated disease-free survival for the 2 groups by the Kaplan-Meier method and compared it by using a logrank test. A P value $<.05$ was considered significant. Hazard ratio and 95% CI were calculated for each parameter.

A subanalysis was performed to assess the bias introduced by neck dissection on disease-free survival. In this analysis, we separated the patients into 2 categories: 1 without neck dissection and another with neck dissection. Using neck dissection as an analytical parameter, we estimated disease-free survival between these 2 categories by the Kaplan-Meier method and compared it by using a logrank test. A P value $< .05$ was considered significant. Hazard ratio and 95% CI were calculated. All data analyses were performed by using a statistical tool (Statistical Package for the Social Sciences for Windows, Version 15.0; SPSS, Chicago, Illinois).

Results

The median pretreatment K^{trans} from 57 patients was 0.41 minutes^{-1} and was used as the threshold K^{trans} value. Of these 57 patients, 29 had K^{trans} values at or higher than the median K^{trans}, and 3 patients died in this group during follow-up. The mean K^{trans} value of these 29 patients was 0.79 ± 0.39 minutes^{-1} with a median of 0.68 minutes^{-1}. On the other hand, K^{trans} values lower than the median K^{trans} were observed in 28 patients, and 10 patients died in this group, with a mean K^{trans} value of 0.17 ± 0.09 minutes^{-1} and a median of 0.15 minutes^{-1}. Univariate analysis revealed that patients with higher K^{trans} values had significantly prolonged disease-free survival compared with patients with lower K^{trans} values ($P = .029$, Fig 2). The hazard ratio was 3.81 (95% CI, 1.04–13.87).

The median pretreatment nodal volume was 13.45 cm^3, and 7 of 29 patients died in the group that had nodal volumes at or higher than the threshold value (mean volume = 32.13 ± 19.2 cm^3, median = 28.25 cm^3). In patients with lower than threshold nodal volumes ($n = 28$), 6 patients died during the

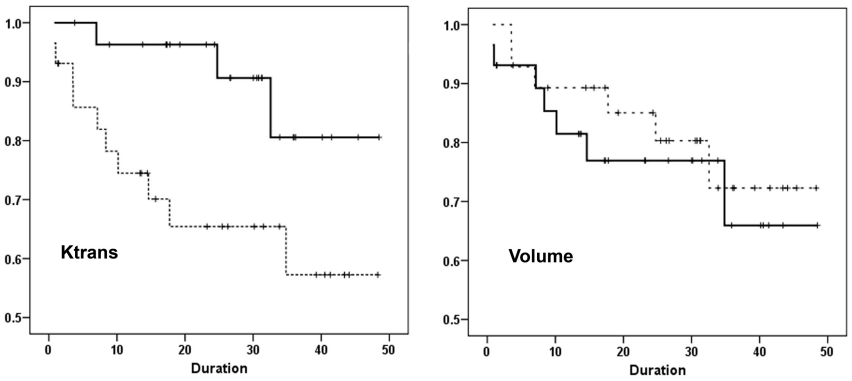

Fig 2. Patients with higher pretreatment K^{trans} values (solid line) demonstrate significantly prolonged disease-free survival compared with patients with lower K^{trans} values (dashed line, $P = .029$). Patients with lower pretreatment nodal volume demonstrate better disease-free survival (dashed line) in comparison with patients with higher nodal volume (solid-line); however, the difference is not significant ($P = .599$). The x-axis shows the follow-up duration in months.

follow-up period. The mean nodal volume in this group was 6.41 ± 3.60 cm^3, with a median volume of 6.83 cm^3. The disease-free survival for patients with lower nodal volumes was not significantly different from that in the patients with higher pretreatment nodal volumes ($P = .599$, Fig 2). The hazard ratio was 0.747 (95% CI, 0.25–2.22).

When a subanalysis was performed to evaluate the bias introduced by neck dissection, no significant difference in the disease-free survival between the patients who underwent neck dissection and patients who did not undergo neck dissection following chemoradiation therapy was observed ($P = .092$). The hazard ratio was 0.365 (95% CI, 0.109–1.22). Of the 24 patients who had neck dissection, 4 patients died, whereas of the 33 patients who did not undergo neck dissection, 9 patients died of HNSCC.

Discussion

Our data indicate that high pretreatment perfusion/permeability of the metastatic HNSCC nodes is significantly associated with better disease-free survival in this patient population. It is often difficult to predict treatment outcome in patients at the time of initial presentation, when critical decisions about selection of the optimal treatment strategy are made. Therefore, identification of risk factors predictive of treatment outcome, as reported in the present study, may aid in identification of high-risk patients who are unlikely to benefit from chemoradiation therapy. These patients can then be considered for alternative experimental therapies.

Several imaging modalities have been proposed for prognosis of treatment response and survival outcome in patients with HNSCC. An earlier study using dynamic CT perfusion parameters did not observe any prognostic significance of tumor perfusion in predicting the cause-specific survival in patients with HNSCC.[6] FDG-PET has shown promising results in predicting the survival rate.[11-13] Using a threshold pretreatment SUV of 9.0 from the primary tumor, Minn et al[11] reported significantly lower survival rates in patients with HNSCC and higher SUVs. These findings have been replicated by several other investigators with a general consensus that elevated baseline SUV of the primary tumor indicates poor local control along with shorter survival.[12,13] However, nodal SUV has not been extensively studied for prediction of survival outcome due to smaller size and complex biologic characteristics responsible for development, growth, and invasiveness of the metastatic nodal masses.[18]

A decrease in FDG uptake from the metastatic node did not correlate with positive survival outcome in patients with HNSCC.[12,13] Moreover, lower spatial resolution of images and problems with discriminating neoplastic processes from inflammation, reactive lymph nodes, obstructive glands, brown fat, or vascular abnormalities lead to false-positive SUVs from the nodal neck region,[14] limiting the use of FDG-PET in evaluating nodal masses. Therefore, alternative imaging methods that can evaluate nodal tumor physiology should be considered.

The relatively higher resolution obtained by DCE-MRI promises to be a powerful tool in assessing tumor hemodynamics with higher sensitivity and specificity. The K^{trans} parameter reflects a combination of tumor blood flow and microvascular permeability.[19] Several studies have reported the use of DCE-MRI in patients with HNSCC for assessment of local treatment response, indicating that tumors with elevated baseline blood flow/blood volume demonstrate a favorable response to therapy.[7,9,10] Hoskin et al[9] reported a good correlation between local tumor control and maximum tumor enhancement following accelerated radiation therapy in patients with advanced head and neck cancer. In a related study, Zima et al[7] reported that patients with higher pretreatment blood volume and blood flow measurements from the primary tumor demonstrated better response and reduction in tumor volume after induction chemotherapy. Cao et al[8] observed a significant increase in tumor blood volume during the early course of chemoradiation therapy in patients who exhibited local control but there was no change in blood volume in patients who demonstrated local failure from chemoradiation. These studies focused only on prediction of short-term local therapeutic response, and there is no evidence to support the prognostic value of DCE-MRI in predicting long-term survival in HNSCC, which may be different from the short-term response.

DCE-MRI has also been used to predict long-term survival in patients with high-grade gliomas, small cell lung cancer, and breast and cervical cancer.[20-23] Loncaster et al[24] reported that patients with cervical cancer with high pretreatment contrast enhancement had significantly improved disease-free survival after radiation therapy. In a recent study, higher base-

line K^{trans} values were reported to have a significant association with progression-free survival in patients with renal cell carcinoma undergoing sorafenib therapy.[25] These studies indicate that higher pretreatment tumor K^{trans} values may predict prolonged survival. Our results are in agreement with these studies in that we also observed that higher pretreatment K^{trans} of the nodal mass predicted longer survival in patients with HNSCC.

The biologic basis for any tumor with a high baseline perfusion to exhibit better prognosis or response to radiation therapy remains largely speculative. Because tumor oxygenation has been shown to influence the radiosensitivity of HNSCC,[26] it can be intuitively postulated that poor baseline nodal perfusion is associated with nodal radioresistance and poor survival as observed in the present study. Tumor vasculature and oxygenation are critical factors that markedly influence the efficacy of chemoradiation therapies, particularly those depending on cell cycle and free radical formation.[27] It is hypothesized that higher tumor blood flow will result in better oxygenation and drug delivery to the target site.[28] On the other hand, hypoxia (decreased blood flow) enhances chemoresistance and impedes delivery of therapeutic agents.[29]

However, the relationship between HNSCC perfusion and hypoxia may be complex as recently described by several investigators[30,31] who used dynamic [^{18}F]fluoromisonidazole PET to assess the perfusion of the primary tumor while simultaneously assessing tumor hypoxia through misonidazole binding. These investigators demonstrated that HNSCC tumors might have significant heterogeneous regions characterized by various perfusion-oxygenation relationships. These include regions characterized by poor perfusion with high levels of hypoxia, regions with high perfusion with very little detectable hypoxia, and even areas of good tumor perfusion along with hypoxia. Tumors with high perfusion can be associated with functionally hypoxic regions, suggesting that these areas may not significantly contribute to an adverse prognosis through a stress response. Alternatively, these regions have been shown to represent areas that may be more apt to undergo successful radiation therapy–induced reoxygenation.[32]

Increased disease-free survival in patients with higher K^{trans}, as observed in the present study, may be explained by the fact that a tumor with elevated blood flow and permeable vasculature has higher oxygenation levels, resulting in better access to chemotherapeutic drugs[28] and radiosensitivity.[33] On the other hand, lower K^{trans} values indicate a heterogeneous blood supply and poor survival. The insufficient blood flow and inadequate oxygen supply result in stabilization and overexpression of hypoxia-inducible factor-1α.[34] These tumors may also exhibit high interstitial fluid pressure and sluggish perfusion with regions of hypoxia, fibrosis, and acidosis.[35] The abnormal hemodynamic environment of such tumors may render them less sensitive to cancer therapies.[35] It has also been reported that hypoxic squamous carcinoma cells show resistance to radiation therapy, cytostatic drugs, and conventional surgery.[36] Taken together, these observations provide evidence that the higher degree of hypoxia and lower perfusion rate, as reflected by low pretreatment K^{trans} from the nodal mass, may indicate an adverse tumor microenvironment and, subsequently, poor survival, as observed in the present study.

Preclinical studies in animal tumor models suggest that improvement in blood flow and pruning of immature functionally abnormal vessel sprouts may enhance the delivery of cytotoxic agents, with subsequent increases in the efficacy of chemotherapy and radiation therapy.[37,38] Initial clinical trials in patients with advanced-stage head and neck cancers treated with bevacizumab reported improved survival.[39] These early results substantiate the hypothesis that vascular normalization and improvement in the blood supply to the tumor can result in an improvement in therapeutic efficacy and survival outcome.

We did not observe a significant relationship between initial nodal volume and disease-free survival, though patients with larger nodal masses tended to show lower disease-free survival. Typically, large and bulky nodal masses are heterogeneous, with a higher degree of necrosis. Thus, it may be more difficult to deliver chemotherapeutic agents to these masses because they might have outstretched their blood supply. Some studies have indicated that the volume of the primary tumor correlates with treatment outcome in patients with advanced HNSCC with the exception of oropharyngeal tumors.[40,41] However, it is unclear whether nodal volume predicts survival in patients with head and neck cancers. While some studies suggested deteriorating regional control[42,43] and worse disease-specific survival[44] in patients with large nodes, other studies did not find any relationship between nodal volume and disease-specific survival.[45,46] These contradictory studies indicate that measurement of tumor volume may not be sensitive in predicting the long-term prognosis and survival in patients with HNSCC. On the other hand, physiologically sensitive parameters such as K^{trans} might be more useful.

Lymphadenopathy in the neck is a well-established and most significant determinant of prognosis in patients with HNSCC; therefore, we focused on the K^{trans} value of the metastatic node for prediction of disease-free survival in patients with HNSCC. However, a similar analysis of tumors at the primary site would also be important, and future studies may be needed to assess the utility of K^{trans} values from the primary tumor in predicting survival in patients with HNSCC. In the present study, we did not assess the potential of nodal staging, performance status, or molecular markers in predicting survival outcome in patients with HNSCC although these parameters could also affect survival. In the present study, >90% of the patients had an N2 stage; thus, we did not have the variance and power to assess the role of nodal staging as a predictor of survival. Some studies have reported patients with similar clinical prognostic features exhibiting variable responses and survival rates.[47,48] Therefore, alternate parameters that can stratify patients for optimal treatment protocol are desirable, and we believe that K^{trans} derived from DCE-MRI can be 1 such parameter.

In clinical settings, assessment of treatment strategy is made with the curative intent of patients in mind. In the present study, even though all patients received the same dose and regimen of radiation therapy, some patients underwent neck dissection within 6 months after chemoradiation therapy, while others were treated with chemoradiation therapy alone and did not undergo neck dissection. Also the patients under-

went different chemotherapy doses and regimens. These differences in treatment may play a confounding role in disease-free survival analysis. To test the bias of neck dissection in predicting disease-free survival, we performed a subanalysis of patients without neck dissection and with neck dissection. When neck dissection was used to predict disease-free survival between patients who underwent neck dissection and patients who did not undergo dissection, irrespective of pretreatment K^{trans} and nodal volume values, no significant difference in disease-free survival between the 2 groups of patients was observed ($P = .092$). This finding indicates that neck dissection does not have an influence on the disease-free survival in our cohort of patients.

Conclusions

Our data suggest that patients with HNSCC with higher pretreatment K^{trans} values from the metastatic lymph nodes respond well to chemoradiation therapy, leading to better disease-free survival; thus, this parameter may be used for better stratification of nonresponsive patients for alternative treatment strategies.

Acknowledgments

The support of MR imaging coordinator Alex Kilger and technologists Doris Cain, Tonya Kurtz, and Patricia O' Donnell is gratefully acknowledged. We also thank Mark Rosen, MD, Department of Radiology, University of Pennsylvania, for his invaluable and helpful suggestions during the preparation of this manuscript.

References

1. Funk GF, Karnell LH, Robinson RA, et al. **Presentation, treatment, and outcome of oral cavity cancer: a National Cancer Data Base report.** *Head Neck* 2002;24:165–80
2. Parkin DM, Bray F, Ferlay J, et al. **Global cancer statistics, 2002.** *CA Cancer J Clin* 2005;55:74–108
3. Layland MK, Sessions DG, Lenox J. **The influence of lymph node metastasis in the treatment of squamous cell carcinoma of the oral cavity, oropharynx, larynx, and hypopharynx: N0 versus N+.** *Laryngoscope* 2005;115:629–39
4. McGurk M, Chan C, Jones J, et al. **Delay in diagnosis and its effect on outcome in head and neck cancer.** *Br J Oral Maxillofac Surg* 2005;43:281–84
5. Gandhi D, Chepeha DB, Miller T, et al. **Correlation between initial and early follow-up CT perfusion parameters with endoscopic tumor response in patients with advanced squamous cell carcinomas of the oropharynx treated with organ-preservation therapy.** *AJNR Am J Neuroradiol* 2006;27:101–06
6. Hermans R, Meijerink M, Van den Bogaert W, et al. **Tumor perfusion rate determined noninvasively by dynamic computed tomography predicts outcome in head-and-neck cancer after radiotherapy.** *Int J Radiat Oncol Biol Phys* 2003;57:1351–56
7. Zima A, Carlos R, Gandhi D, et al. **Can pretreatment CT perfusion predict response of advanced squamous cell carcinoma of the upper aerodigestive tract treated with induction chemotherapy?** *AJNR Am J Neuroradiol* 2007;28:328–34
8. Cao Y, Popovtzer A, Li D, et al. **Early prediction of outcome in advanced head-and-neck cancer based on tumor blood volume alterations during therapy: a prospective study.** *Int J Radiat Oncol Biol Phys* 2008;72:1287–90
9. Hoskin PJ, Saunders MI, Goodchild K, et al. **Dynamic contrast enhanced magnetic resonance scanning as a predictor of response to accelerated radiotherapy for advanced head and neck cancer.** *Br J Radiol* 1999;72:1093–98
10. Kim S, Loevner LA, Quon H, et al. **Prediction of response to chemoradiation therapy in squamous cell carcinomas of the head and neck using dynamic contrast-enhanced MR imaging**. *AJNR Am J Neuroradiol* 2010;31:262–68. Epub 2009 Oct 1
11. Minn H, Lapela M, Klemi PJ, et al. **Prediction of survival with fluorine-18-fluoro-deoxyglucose and PET in head and neck cancer.** *J Nucl Med* 1997;38:1907–11
12. Schwartz DL, Rajendran J, Yueh B, et al. **FDG-PET prediction of head and neck squamous cell cancer outcomes.** *Arch Otolaryngol Head Neck Surg* 2004;130:1361–67
13. Brun E, Kjellen E, Tennvall J, et al. **FDG PET studies during treatment: prediction of therapy outcome in head and neck squamous cell carcinoma.** *Head Neck* 2002;24:127–35
14. McCollum AD, Burrell SC, Haddad RI, et al. **Positron emission tomography with 18F-fluorodeoxyglucose to predict pathologic response after induction chemotherapy and definitive chemoradiotherapy in head and neck cancer.** *Head Neck* 2004;26:890–96
15. Kim S, Quon H, Loevner LA, et al. **Transcytolemmal water exchange in pharmacokinetic analysis of dynamic contrast-enhanced MRI data in squamous cell carcinoma of the head and neck.** *J Magn Reson Imaging* 2007;26:1607–17
16. Song HK, Dougherty L. **Dynamic MRI with projection reconstruction and KWIC processing for simultaneous high spatial and temporal resolution.** *Magn Reson Med* 2004;52:815–24
17. Kim S, Dougherty L, Rosen MA, et al. **Automatic correction of in-plane bulk motion artifacts in self-navigated radial MRI.** *Magn Reson Imaging* 2008;26:367–78
18. Wennerberg J. **Predicting response to therapy of squamous cell carcinoma of the head and neck (review).** *Anticancer Res* 1996;16:2389–96
19. Tofts PS, Brix G, Buckley DL, et al. **Estimating kinetic parameters from dynamic contrast-enhanced T(1)-weighted MRI of a diffusable tracer: standardized quantities and symbols.** *J Magn Reson Imaging* 1999;10:223–32
20. Hawighorst H, Knapstein PG, Knopp MV, et al. **Uterine cervical carcinoma: comparison of standard and pharmacokinetic analysis of time-intensity curves for assessment of tumor angiogenesis and patient survival.** *Cancer Res* 1998;58:3598–602
21. Bone B, Szabo BK, Perbeck LG, et al. **Can contrast-enhanced MR imaging predict survival in breast cancer?** *Acta Radiol* 2003;44:373–78
22. Ohno Y, Nogami M, Higashino T, et al. **Prognostic value of dynamic MR imaging for non-small-cell lung cancer patients after chemoradiotherapy.** *J Magn Reson Imaging* 2005;21:775–83
23. Mills SJ, Patankar TA, Haroon HA, et al. **Do cerebral blood volume and contrast transfer coefficient predict prognosis in human glioma?** *AJNR Am J Neuroradiol* 2006;27:853–58
24. Loncaster JA, Carrington BM, Sykes JR, et al. **Prediction of radiotherapy outcome using dynamic contrast-enhanced MRI of carcinoma of the cervix.** *Int J Radiat Oncol Biol Phys* 2002;54:759–67
25. Flaherty KT, Rosen MA, Heitjan DF, et al. **Pilot study of DCE-MRI to predict progression-free survival with sorafenib therapy in renal cell carcinoma.** *Cancer Biol Ther* 2008;7:496–501
26. Le QT, Kovacs MS, Dorie MJ, et al. **Comparison of the comet assay and the oxygen microelectrode for measuring tumor oxygenation in head-and-neck cancer patients.** *Int J Radiat Oncol Biol Phys* 2003;56:375–83
27. Vaupel P, Kallinowski F, Okunieff P. **Blood flow, oxygen and nutrient supply, and metabolic microenvironment of human tumors: a review.** *Cancer Res* 1989;49:6449–65
28. Cooper RA, Carrington BM, Loncaster JA, et al. **Tumour oxygenation levels correlate with dynamic contrast-enhanced magnetic resonance imaging parameters in carcinoma of the cervix.** *Radiother Oncol* 2000;57:53–59
29. Cosse JP, Michiels C. **Tumour hypoxia affects the responsiveness of cancer cells to chemotherapy and promotes cancer progression.** *Anticancer Agents Med Chem* 2008;8:790–97
30. Thorwarth D, Eschmann SM, Scheiderbauer J, et al. **Kinetic analysis of dynamic 18F-fluoromisonidazole PET correlates with radiation treatment outcome in head-and-neck cancer.** *BMC Cancer* 2005;5:152
31. Jansen JF, Schöder H, Lee NY, et al. **Noninvasive assessment of tumor microenvironment using dynamic contrast-enhanced magnetic resonance imaging and 18F- fluoromisonidazole positron emission tomography imaging in neck nodal metastases**. *Int J Radiat Oncol Biol Phys* 2010;77:1403–10. Epub 2009 Nov 10
32. Thorwarth D, Eschmann SM, Paulsen F, et al. **A model of reoxygenation dynamics of head-and-neck tumors based on serial 18F-fluoromisonidazole positron emission tomography investigations.** *Int J Radiat Oncol Biol Phys* 2007;68:515–21
33. Protopapa E, Delides GS, Revesz L. **Vascular density and the response of breast carcinomas to mastectomy and adjuvant chemotherapy.** *Eur J Cancer* 1993;29A:1391–93
34. Gruber M, Simon MC. **Hypoxia-inducible factors, hypoxia, and tumor angiogenesis.** *Curr Opin Hematol* 2006;13:169–74
35. Yang AD, Bauer TW, Camp ER, et al. **Improving delivery of antineoplastic agents with anti-vascular endothelial growth factor therapy.** *Cancer* 2005;103:1561–70
36. Lutterbach J, Guttenberger R. **Anemia is associated with decreased local control of surgically treated squamous cell carcinomas of the glottic larynx.** *Int J Radiat Oncol Biol Phys* 2000;48:1345–50
37. Wildiers H, Guetens G, De Boeck G, et al. **Effect of antivascular endothelial growth factor treatment on the intratumoral uptake of CPT-11.** *Br J Cancer* 2003;88:1979–86
38. Tong RT, Boucher Y, Kozin SV, et al. **Vascular normalization by vascular endothelial growth factor receptor 2 blockade induces a pressure gradient across**

the vasculature and improves drug penetration in tumors. *Cancer Res* 2004;64:3731–36
39. Fujita K, Sano D, Kimura M, et al. **Anti-tumor effects of bevacizumab in combination with paclitaxel on head and neck squamous cell carcinoma.** *Oncol Rep* 2007;18:47–51
40. Mendenhall WM, Parsons JT, Mancuso AA, et al. **Radiotherapy for squamous cell carcinoma of the supraglottic larynx: an alternative to surgery.** *Head Neck* 1996;18:24–35
41. Been MJ, Watkins J, Manz RM, et al. **Tumor volume as a prognostic factor in oropharyngeal squamous cell carcinoma treated with primary radiotherapy.** *Laryngoscope* 2008;118:1377–82
42. Hermans R, Op de beeck K, Van den Bogaert W, et al. **The relation of CT-determined tumor parameters and local and regional outcome of tonsillar cancer after definitive radiation treatment.** *Int J Radiat Oncol Biol Phys* 2001;50:37–45
43. Vergeer MR, Doornaert P, Leemans CR, et al. **Control of nodal metastases in squamous cell head and neck cancer treated by radiation therapy or chemoradiation.** *Radiother Oncol* 2006;79:39–44
44. Kim JH, Lee JK. **Prognostic value of tumor volume in nasopharyngeal carcinoma.** *Yonsei Med J* 2005;46:221–27
45. Doweck I, Denys D, Robbins KT. **Tumor volume predicts outcome for advanced head and neck cancer treated with targeted chemoradiotherapy.** *Laryngoscope* 2002;112:1742–49
46. Chua DT, Sham JS, Leung LH, et al. **Tumor volume is not an independent prognostic factor in early-stage nasopharyngeal carcinoma treated by radiotherapy alone.** *Int J Radiat Oncol Biol Phys* 2004;58:1437–44
47. Thomas GR, Nadiminti H, Regalado J. **Molecular predictors of clinical outcome in patients with head and neck squamous cell carcinoma.** *Int J Exp Pathol* 2005;86(6):347–63
48. Wendt TG, Bank P. **Prognostic factors in squamous cell carcinoma of the head and neck.** *Onkologie* 2002;25:208–12